Applied Physics Letters

First and second order rotational transitions of skyrmion crystal in multiferroic Cu_2OSeO_3 under electric field

Cite as: Appl. Phys. Lett. **116**, 182403 (2020); https://doi.org/10.1063/5.0003880
Submitted: 05 February 2020 . Accepted: 20 April 2020 . Published Online: 04 May 2020

Xuejin Wan, Yangfan Hu, and Biao Wang

Applied Physics Letters ARTICLE scitation.org/journal/apl

First and second order rotational transitions of skyrmion crystal in multiferroic Cu_2OSeO_3 under electric field

Cite as: Appl. Phys. Lett. **116**, 182403 (2020); doi: 10.1063/5.0003880
Submitted: 5 February 2020 · Accepted: 20 April 2020 ·
Published Online: 4 May 2020

View Online Export Citation CrossMark

Xuejin Wan, Yangfan Hu,[a] and Biao Wang[a]

AFFILIATIONS

Sino-French Institute of Nuclear Engineering and Technology, Sun Yat-sen University, 519082 Zhuhai, China

[a]Authors to whom correspondence should be addressed: huyf3@mail.sysu.edu.cn and wangbiao@mail.sysu.edu.cn

ABSTRACT

We investigate the electric-field-induced rotations of a skyrmion crystal (SkX) in multiferroic Cu_2OSeO_3. We perform our analysis within a free energy model that incorporates both the exchange anisotropy and the fourth order magnetocrystalline anisotropy, and both the deformation and rotation of SkX are taken into account. We find that for a background magnetic field along the direction [110], (i) electric fields out of the $(1\bar{1}0)$ plane lead to continuous rotations of SkX, which explains the experiments [White *et al.*, Phys. Rev. Lett. **113**, 107203 (2014)] and (ii) electric fields in the $(1\bar{1}0)$ plane may lead to 30° rotations of SkX. Our results provide an understanding of manipulation of SkX by the electric field, which may contribute to the applications of skyrmion-based spintronic devices without Joule heating energy losses.

Magnetic skyrmions, topologically protected spin textures, have been attracting great interest since their first observation a decade ago.[1] Due to their small size, topological stability, and facile current driven motion,[2,3] magnetic skyrmions are very promising for spintronic applications, such as high density storage devices and low energy consuming memories.[4] In noncentrosymmetric helimagnets, the antisymmetric Dzyaloshinskii–Moriya interaction (DMI) arises due to the breakage of spatial inverse symmetry.[5] It competes with the Heisenberg exchange interaction and results in the SkX. The symmetry of the helimagnets dictates the form of DMI and thus the spin distribution of SkX.[6] SkX is Bloch type in MnSi,[1] FeGe,[7] $Fe_{1-x}Co_xSi$,[8] Cu_2OSeO_3[9,10] (T point group), and β-Mn-type Co–Zn–Mn alloy[11] (O point group); it is Néel type in GaV_4S_8,[12] GaV_4Se_8[13] (C_{3v} point group), $VOSe_2O_5$[14] (C_{4v} point group), and $Y_3Co_8Sn_4$[15] (C_{6v} point group); and it is Anti-type in $Mn_{1.4}Pt_{0.9}Pd_{0.1}Sn$[16] ($D_{2d}$ point group).

Among the helimagnets hosting skyrmions, Cu_2OSeO_3 has some fascinating features. First, Cu_2OSeO_3 permits some uncommon magnetic phases, the tilted conical phase and the low temperature skyrmion phase.[17–20] Second, Cu_2OSeO_3 is multiferroic, meaning that apart from the widely used magnetic field,[21,22] strain field,[23] and thermal gradient field,[24] the electric field can be applied to manipulate skyrmions.[25–28] For instance, it has been found that the electric field can induce the rotation of SkX.[25,29]

In the phenomena of Cu_2OSeO_3 mentioned above, including the appearance of new magnetic phases,[17–20] and the rotation of SkX under the electric field,[25,29] the fourth order magnetocrystalline anisotropy [see Eq. (3)] plays an important role. According to Refs. 17–20, it should be negative. However, the model in Ref. 29 needs it to be positive to explain the rotation of SkX under the electric field. This encourages us to establish another model to explain the electric-field-induced rotation of SkX.

Different from the perturbation model,[1,30,31] we treat SkX as deformable and describe SkX by a three-order Fourier expansion with deformation-related degrees of freedom. The anisotropies considered are those of fourth order in spin–orbit coupling, and they are the exchange and the fourth order magnetocrystalline anisotropies. When no electric field is applied, it is found that anisotropies can induce deformation and pinning of SkX; such effects of anisotropies on SkX are ignored in previous works.[1,29–31] By plotting the azimuthal angle of a wave vector of SkX as a function of the electric field, the fourth order magnetocrystalline anisotropies with a negative coefficient together with the exchange anisotropy can reproduce the continuous rotation of SkX observed in experiments. Then, if we change the direction of the electric field, 30° rotations of SkX are observed for certain directions.

We apply the following continuum model to describe the rescaled free energy density[6,32] of the multiferroic helimagnets Cu_2OSeO_3:

$$\omega(\mathbf{m}) = \sum_{i=1}^{3}\left(\frac{\partial \mathbf{m}}{\partial r_i}\right)^2 + 2\mathbf{m}\cdot(\nabla\times\mathbf{m}) - 2\mathbf{b}\cdot\mathbf{m} + \omega_{\mathrm{L}}(\mathbf{m}) + \omega_{\mathrm{me}}(\mathbf{m}) + \omega_{\mathrm{a}}(\mathbf{m}). \quad (1)$$

Here, $\mathbf{m} = [m_1, m_2, m_3]^{\mathrm{T}}$ is the rescaled magnetization in the frame O-$r_1r_2r_3$. The gradient terms in Eq. (1) represent the Heisenberg exchange interaction and the DMI, respectively. They are responsible for the occurrence of chiral phases. The third term is the Zeeman interaction with rescaled magnetic field $\mathbf{b}$. ω_{L} is the Landau expansion, and it consists of the second-order term $t\mathbf{m}^2$ (t is the rescaled temperature) and the fourth-order terms $\mathbf{m}^4$. ω_{me} is the magnetoelectric coupling. In cubic helimagnets Cu_2OSeO_3, the electric dipole moment depends on the local magnetization configuration and is proportional to $[m_2m_3,\ m_1m_3,\ m_1m_2]^{\mathrm{T}}$.[26,33,34] As a result, the magnetoelectric coupling can be expressed as

$$\omega_{\mathrm{me}} = -(e_1m_2m_3 + e_2m_1m_3 + e_3m_1m_2), \quad (2)$$

where $\mathbf{e} = [e_1, e_2, e_3]^{\mathrm{T}}$ is the rescaled external electric field.[29,35] The last term in Eq. (1) is the anisotropy energy density. In this work, we consider only anisotropies of fourth order in spin–orbit coupling and write ω_a as

$$\omega_{\mathrm{a}} = a_{\mathrm{e}1}\sum_{i=1}^{3}\left(\frac{\partial m_i}{\partial r_i}\right)^2 + a_{\mathrm{e}2}\sum_{i=1}^{3}\left(\frac{\partial m_i}{\partial r_{i+1}}\right)^2 + a_{\mathrm{e}3}\sum_{i=1}^{3}\left(\frac{\partial m_i}{\partial r_{i-1}}\right)^2 + a_{\mathrm{m}}\sum_{i=1}^{3} m_i^4, \quad (3)$$

where $a_{\mathrm{e}i}\ (i = 1, 2, 3)$ and a_{m} are the coefficients of the exchange anisotropy and the fourth order magnetocrystalline anisotropy, respectively; r_{3+1} and r_{1-1} represent r_1 and r_3, respectively.

We now choose a new frame O-$r_1^*r_2^*r_3^*$ in which the magnetic field is along the r_3^* axis. Let the azimuthal and polar angles of $\mathbf{b}$ in the O-$r_1r_2r_3$ frame be θ and ψ, respectively. The O-$r_1^*r_2^*r_3^*$ frame is obtained by

$$O - r_1r_2r_3 \xrightarrow{R_{r_3}(\theta)} O - r_1'r_2'r_3' \xrightarrow{R_{r_2'}(\psi)} O - r_1^*r_2^*r_3^*,$$

where $R_{r_3}(\theta)$ ($R_{r_2'}(\psi)$) stands for the rotation about the r_3 (r_2') axis by angle θ (ψ). Due to the fact that rotations by the same angle belong to a single class of group SO(3), we have $R_{r_2'}(\psi) = R_{r_3}(\theta)R_{r_2}(\psi)R_{r_3}^{-1}(\theta)$. Therefore, $R(\theta,\psi) = R_{r_2'}(\psi)R_{r_3}(\theta) = R_{r_3}(\theta)R_{r_2}(\psi)$.

In the new frame O-$r_1^*r_2^*r_3^*$, the magnetization texture of SkX is described by the three-order Fourier decomposition (for detailed information, see our previous works[6,21,32])

$$\mathbf{m}^* = \mathbf{m}_0 + \sum_{i=1}^{3}\sum_{j=1}^{n_i}\mathbf{m}_{\mathbf{q}_{ij}}\mathrm{e}^{\mathrm{i}\mathbf{q}_{ij}^{\mathrm{d}}\cdot\mathbf{r}^*}. \quad (4)$$

Here, $\mathbf{m}_0 = [m_{01}, m_{02}, m_{03}]^{\mathrm{T}}$ is the mean magnetization. i represents the order of Fourier series, and n_i is the number of the ith order waves; we have $n_1 = n_2 = n_3 = 6$. $\mathbf{q}_{ij}^{\mathrm{d}}$ are the wave vectors of the ith order waves; according to the Cauchy–Born law,[36] they can be written as

$$\mathbf{q}_{ij}^{\mathrm{d}} = \begin{bmatrix} 1+\varepsilon_{11}^q & \varepsilon_{12}^q + \omega^q \\ \varepsilon_{12}^q - \omega^q & 1+\varepsilon_{22}^q \end{bmatrix}\mathbf{q}_{ij}, \quad (5)$$

where ε_{11}^q, ε_{12}^q, ε_{22}^q, and ω^q describe the strains and rotation of the reciprocal lattices of the SkX in the $r_1^*r_2^*$-plane, and $\mathbf{q}_{ij}$ are the undeformed wave vectors (without loss of generality, for hexagonal SkX, we set $\mathbf{q}_{11} = [0,\ 1]^{\mathrm{T}}$, $\mathbf{q}_{12} = [-\frac{\sqrt{3}}{2}, -\frac{1}{2}]^{\mathrm{T}}$). $\mathbf{m}_{\mathbf{q}_{ij}}$ are the polarization vectors of the ith order waves, and they can be decomposed in an orthonormal basis as

$$\mathbf{m}_{\mathbf{q}_{ij}} = \sum_{k=1}^{3} c_{ijk}\mathbf{P}_{ijk}, \quad (6)$$

where $c_{ijk} = c_{ijk}^{\mathrm{re}} + \mathrm{i}c_{ijk}^{\mathrm{im}}\ (k = 1, 2, 3)$ are the complex coefficients and $\mathbf{P}_{ijk}$ are the basis vectors whose values depend on the type of DMI. For Bloch-type DMI in B20 helimagnets, $\mathbf{P}_{ij1} = \frac{1}{\sqrt{2}|\mathbf{q}_{ij}|}[-\mathrm{iq_{ijy}},\ \mathrm{iq_{ijx}},\ |\mathbf{q}_{ij}|]^{\mathrm{T}}$, $\mathbf{P}_{ij2} = \frac{1}{|\mathbf{q}_{ij}|}[\mathrm{q_{ijx}},\ \mathrm{q_{ijy}},\ 0]^{\mathrm{T}}$, and $\mathbf{P}_{ij3} = \frac{1}{\sqrt{2}|\mathbf{q}_{ij}|}[\mathrm{iq_{ijy}},\ -\mathrm{iq_{ijx}},\ |\mathbf{q}_{ij}|]^{\mathrm{T}}$.[6]

According to Eqs. (1)–(3), the free energy density is a functional of m_i and $m_{j,k}$ ($m_{j,k} \equiv \frac{\partial m_j}{\partial r_k}$), i.e., $\omega = \omega(m_i,\ m_{j,k})$. Since $\mathbf{m}$ is a first order tensor and $\nabla\mathbf{m}$ is a second order tensor, we have, under rotation $R(\theta,\psi)$,

$$\begin{aligned} m_i &= \sum_{i'=1}^{3} R(\theta,\psi)_{ii'} m_{i'}^*, \\ m_{j,k} &= \sum_{j',k'=1}^{3} R(\theta,\psi)_{jj'}R(\theta,\psi)_{kk'} m_{j',k'}^*. \end{aligned} \quad (7)$$

Substituting Eq. (7) into Eq. (1) and averaging over a magnetic unit cell, the free energy density can be rewritten as

$$\omega = \omega(\varepsilon_{11}^q, \varepsilon_{22}^q, \varepsilon_{12}^q, \omega_{11}^q, m_{01}, m_{02}, m_{03}, c_{ijk}^{\mathrm{re}}, c_{ijk}^{\mathrm{im}}). \quad (8)$$

At certain conditions, we calculate the parameters describing SkX via minimization of Eq. (8).

At first, we study the reorientation of SkX induced by the electric field without considering any anisotropies. The magnetic field is applied along the [110] direction by setting the angles $\theta = 45°$ and $\psi = 90°$. The electric field is applied along the $[\bar{1}11]$ direction (negative direction for $\mathbf{e}$) or the $[1\bar{1}\bar{1}]$ direction. In this case, the geometry is equivalent to the experiments in which $\mathbf{b}||[1\bar{1}0]$ and $\mathbf{e}||[111]$.[29] The value of $\mathbf{e}$ varies from −0.006 to 0.006, which corresponds to the electric field about several kV/mm.[29,35] The temperature $t = 0$ and the magnetic field $b = 0.2$ are chosen so that SkX exists as a stable or metastable state. φ_{11}, the angle between the wave vector $\mathbf{q}_{11}^{\mathrm{d}}$ and the axis r_1^*, as a function of the rescaled electric field e is plotted in Fig. 1(a) (see the blue curve). The result shows that with increasing e, φ_{11} varies in a range of 30°, from 65° ($-0.006 < e < -0.0035$) to 95° ($0.0021 < e < 0.006$) and that at zero electric field $\varphi_{11} = 90°$, i.e., $\mathbf{q}_{11}^{\mathrm{d}}||[110]$. This does not match with the experiments, in which the rotation range of SkX is smaller than 30° and a wave vector is along a $\langle 100\rangle$ direction for $e = 0$.[29]

To reproduce the electric-field-induced second order rotation of SkX in experiments, anisotropies should be taken into account. The first candidate is the fourth order magnetocrystalline anisotropy, which is widely applied to explain the pinning of the helix at zero magnetic field and the occurrence of new phases.[17–20] Figure 1(a) shows the SkX rotation as a function of electric field for different magnetocrystalline anisotropies a_{m}. It can be found that (i) for a negative a_{m}, φ_{11} increases monotonically with e, while for a positive a_{m}, the

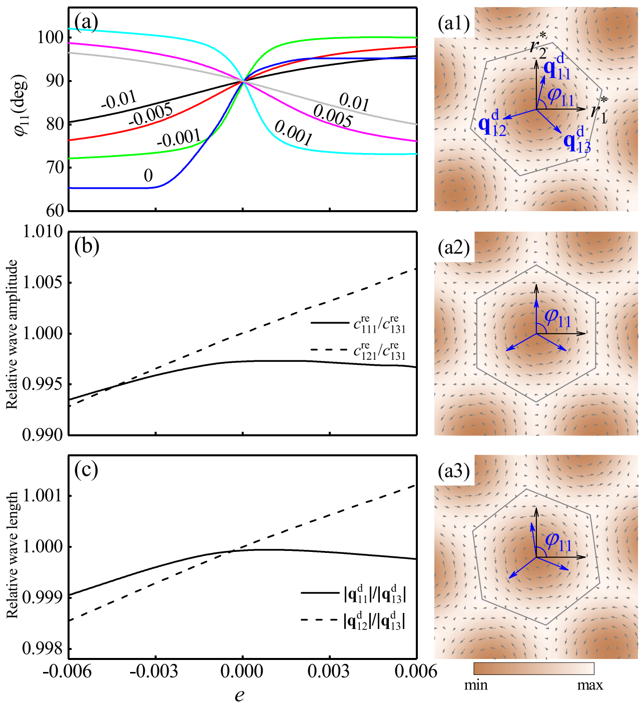

FIG. 1. (a) The electric field dependence of the angle φ_{11} between the wave vector $\mathbf{q}_{11}^{\mathrm{d}}$ and the axis r_1^* for different magnetocrystalline anisotropies a_{m} (from -0.01 to 0.01). (a1)–(a3) show the configuration of SkX at $a_{\mathrm{m}} = -0.005$ and $e = -0.006$, 0, and 0.006, respectively. The hexagon represents the Wigner–Seitz cell of SkX. The arrows and the colored density plot illustrate the in-plane and out-of-plane magnetization components, respectively. Here, $\theta = 45^\circ$ and $\psi = 90^\circ$; therefore, $r_1^* \| [00\bar{1}]$ and $r_2^* \| [\bar{1}10]$. Deformation-related parameters of SkX: (b) $c_{111}^{\mathrm{re}}/c_{131}^{\mathrm{re}}$ and $c_{121}^{\mathrm{re}}/c_{131}^{\mathrm{re}}$ and (c) $|\mathbf{q}_{11}^{\mathrm{d}}|/|\mathbf{q}_{13}^{\mathrm{d}}|$ and $|\mathbf{q}_{12}^{\mathrm{d}}|/|\mathbf{q}_{13}^{\mathrm{d}}|$ as functions of the electric field e for $a_{\mathrm{m}} = -0.005$.

opposite is the case; (ii) the rotation range of SkX decreases with increasing strength of a_{m}, from 28° ($a_{\mathrm{m}} = -0.001$) to 22° ($a_{\mathrm{m}} = -0.005$) then to 17° ($a_{\mathrm{m}} = -0.01$); (iii) the rotation induced by a negative e is larger than that induced by a positive e, meaning that the rotations are asymmetric with the electric field; and (iv) the a_{m}, no matter what its sign is, pins SkX with a wave vector along the $[\bar{1}10]$ direction at zero electric field. Figures 1(a1)–(a3) display the configurations of SkX at $a_{\mathrm{m}} = -0.005$ and at different electric fields. Rotations of SkX are obvious, but deformations of SkX are not discerned at present conditions due to their smallness. To reveal these small deformations induced by the electric field and magnetocrystalline anisotropy, we plot Figs. 1(b) and 1(c) that show some deformation-related parameters, such as the relative wave amplitudes $c_{111}^{\mathrm{re}}/c_{131}^{\mathrm{re}}$ and $c_{121}^{\mathrm{re}}/c_{131}^{\mathrm{re}}$ and the relative wavelengths $|\mathbf{q}_{11}^{\mathrm{d}}|/|\mathbf{q}_{13}^{\mathrm{d}}|$ and $|\mathbf{q}_{12}^{\mathrm{d}}|/|\mathbf{q}_{13}^{\mathrm{d}}|$ of the first order waves, as functions of electric field. For SkX with hexagonal symmetry, the waves of the same order are equivalent, i.e., they have the same amplitude and the same length. The deviations of $c_{111}^{\mathrm{re}}/c_{131}^{\mathrm{re}}$, $c_{121}^{\mathrm{re}}/c_{131}^{\mathrm{re}}$, $|\mathbf{q}_{11}^{\mathrm{d}}|/|\mathbf{q}_{13}^{\mathrm{d}}|$, and $|\mathbf{q}_{12}^{\mathrm{d}}|/|\mathbf{q}_{13}^{\mathrm{d}}|$ from 1 characterize the deformation of SkX. According to Figs. 1(b) and 1(c), the range of $c_{121}^{\mathrm{re}}/c_{131}^{\mathrm{re}}$ is about 1 order of magnitude larger than that of $|\mathbf{q}_{12}^{\mathrm{d}}|/|\mathbf{q}_{13}^{\mathrm{d}}|$; therefore, in this case, the deformation of SkX is reflected mainly by the changes in wave amplitudes. At $e = 0$, we have $|1 - c_{121}^{\mathrm{re}}/c_{131}^{\mathrm{re}}| = 0$, $|1 - c_{111}^{\mathrm{re}}/c_{131}^{\mathrm{re}}| \approx 0.003$, and the nonequivalence between the waves $\mathbf{q}_{11}^{\mathrm{d}}$ and $\mathbf{q}_{13}^{\mathrm{d}}$ is induced by the magnetocrystalline anisotropy; at $e = 0.006$, we have $|1 - c_{121}^{\mathrm{re}}/c_{131}^{\mathrm{re}}| \approx 0.007$, $|1 - c_{111}^{\mathrm{re}}/c_{131}^{\mathrm{re}}| \approx 0.004$, and the nonequivalence between the waves $\mathbf{q}_{12}^{\mathrm{d}}$ and $\mathbf{q}_{13}^{\mathrm{d}}$ is induced by the electric field. We can say that deformations induced by the electric field and by magnetocrystalline anisotropy are of the same importance. This is different from previous works[29–31] that ignored totally the deformation induced by intrinsic anisotropies.

Compared to experiments, a negative a_{m} reproduces well the variation trend of φ_{11} with the electric field. However, a negative a_{m} solely cannot explain the pinning of SkX along a $\langle 100 \rangle$ direction at zero electric field. We now resort to another kind of anisotropy, exchange anisotropies. As a first step, we ignore the influence of the magnetocrystalline anisotropy by setting $a_{\mathrm{m}} = 0$ and investigate the effects of exchange anisotropies on SkX rotation. The results are plotted in Fig. 2. The effects of $a_{\mathrm{e}i}$ ($i = 1, 2, 3$) on SkX are the same as those of a_{m} in two aspects. First, the second order rotations with respect to the electric field are asymmetric; second, the larger the strength of the anisotropies is, the smaller the rotation angle is. As to the difference between a_{m} and $a_{\mathrm{e}i}$ ($i = 1, 2, 3$), an a_{m} pins $\varphi_{11} = 90^\circ$ at zero electric field, while an $a_{\mathrm{e}i}$ ($i = 1, 2, 3$) pins $\varphi_{11} = 60^\circ$ at zero electric field, which is just the case in experiments.

Next, we take other experimental facts into account. For Cu_2OSeO_3, the helix appearing at zero magnetic field has a preference for the $\langle 100 \rangle$ directions.[10] To study the pinning effects of anisotropies on the helix, we fix $\theta = 45^\circ$ so that the r_3^* axis is in the $(1\bar{1}0)$ plane, which contains the direction with high symmetry, such as [001], [111], and [110]. Then, we write the magnetization of the helical state in the O-$r_1^* r_2^* r_3^*$ frame as

$$\mathbf{m}_{\mathrm{h}}^* = \left[m_q \cos(q r_3^*),\ m_q \cos(q r_3^*),\ 0\right]^{\mathrm{T}}, \tag{9}$$

where m_q and q are the wave amplitude and wavelength, respectively. Treating the angle ψ as a variable and substituting Eqs. (9) and (7) into Eq. (3), we have, after averaging over a magnetic unit cell,

$$\begin{aligned}\omega_{\mathrm{a}} = &-\frac{3m_q^2 q^2}{4} a_{\mathrm{e}1}\left(\sin^4(\psi) - \frac{4}{3}\sin^2(\psi)\right)\\ &+\frac{3m_q^2 q^2}{8}(a_{\mathrm{e}2} + a_{\mathrm{e}3})\left(\sin^4(\psi) - \frac{4}{3}\sin^2(\psi) + \frac{4}{3}\right)\\ &+\frac{9m_q^4}{16} a_{\mathrm{m}}\left(\sin^4(\psi) - \frac{4}{3}\sin^2(\psi) + \frac{4}{3}\right).\end{aligned} \tag{10}$$

According to Eq. (10), for a positive $a_{\mathrm{e}1}$ (a negative $a_{\mathrm{e}2}$, $a_{\mathrm{e}3}$ or a_{m}), $\sin(\psi) = 0$, i.e., the helix is along the [001] direction, while for a

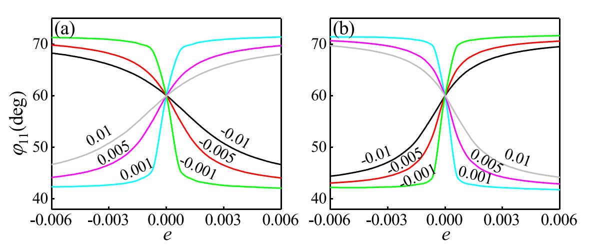

FIG. 2. φ_{11} as a function of the electric field e for different values of (a) $a_{\mathrm{e}1}$ and (b) $a_{\mathrm{e}2}$. The rotation effects of $a_{\mathrm{e}3}$ is the same as those of $a_{\mathrm{e}2}$, and we do not plot $\varphi_{11}(e)$ for $a_{\mathrm{e}3}$.

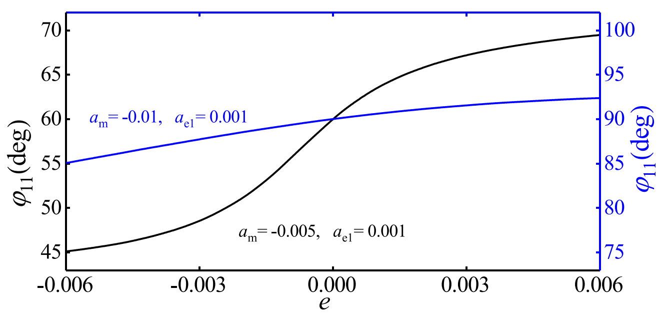

FIG. 3. φ_{11} as a function of the electric field. The black curve is obtained for $a_m = -0.005$ and $a_{e1} = 0.001$, and the blue curve is obtained for $a_m = -0.01$ and $a_{e1} = 0.001$.

negative a_{e1} (a positive a_{e2}, a_{e3} or a_m), $\sin(\psi) = \sqrt{\frac{2}{3}}$, i.e., the helix is along the [111] direction. In Ref. 29, the fourth and sixth order magnetocrystalline anisotropies were applied to explain the second order rotation of SkX under the electric field. However, the coefficient of the fourth order magnetocrystalline anisotropy was positive. This is not reasonable since, in this case, the helix is along the [111] direction, which is inconsistent with the experiments.[10]

Actually, other small-angle neutron scattering and resonant soft x-ray scattering experiments of Cu_2OSeO_3 have shown that when the magnetic field $\mathbf{b}||[110]$, SkX has a wave vector along the [001] or $[\bar{1}10]$ directions depending on the temperature t or the strength of magnetic field b or the thermal history.[37–39] If these are considered, the anisotropies should contain the magnetocrystalline and exchange anisotropies at the same time. As we have revealed before [see Figs. 1(a) and 2], an a_m (a_{ei} ($i = 1, 2, 3$)) prefers a wave vector along the $[\bar{1}10]$ ([001]) direction. We now study the combined effects of magnetocrystalline and exchange anisotropies on SkX under the electric field. We chose negative a_m and positive a_{e1} so that the helix is aligned along a $\langle 100 \rangle$ direction at zero field [see Eq. (10)]. According to Fig. 3 that shows the curves $\varphi_{11}(e)$ for $a_m = -0.005$ and $a_{e1} = 0.001$ (black) and for $a_m = -0.01$ and $a_{e1} = 0.001$ (blue), the magnetocrystalline and exchange anisotropies compete with each other. If the magnetocrystalline anisotropy dominates, $\varphi_{11}(0) = 90°$, while if the exchange anisotropy dominates, $\varphi_{11}(0) = 60°$. We can, therefore, attribute the first order rotation of SkX from [001] to $[\bar{1}10]$ to the competition between the magnetocrystalline and exchange anisotropies.

Finally, we study the rotations of SkX under electric fields with different directions. The temperature and magnetic field conditions remain the same, i.e., $t = 0$, $b = 0.2$ and $\mathbf{b}||[110]$; the anisotropies considered are $a_m = -0.005$ and $a_{e1} = 0.001$. The results are displayed in Fig. 4. Obviously, the electric fields can be classified into two types. Type one results in a continuous change of φ_{11} with e [Figs. 4(a)–4(c)], and type two does not change φ_{11} or results in a sudden jump of φ_{11} [Figs. 4(d)–4(f)]. It can be found that the electric fields of type one (or type two) have a common feature; they are out of (or in) the plane $(1\bar{1}0)$. In the experiments[40] where the geometry is the same as that in Fig. 4(f), no second order rotation of SkX was observed. This was thought to be due to the tensile strain. However, in our point of view, this is just because the electric field is applied in the $(1\bar{1}0)$ plane. Another point we should notice is that if the component of the electric field perpendicular to the plane $(1\bar{1}0)$ is along the $[1\bar{1}0]$ direction, SkX rotates counterclockwise, and otherwise, SkX rotates clockwise. This is also applicable to the previous case where the electric field is along the $[\bar{1}11]$ or $[1\bar{1}\bar{1}]$ direction (Fig. 3). We now give a possible explanation to the 30° jump of φ_{11}. An electric field $\mathbf{e}||[111]$ or $||[001]$ prefers the magnetocrystalline anisotropy. When the electric field is high enough, the magnetocrystalline anisotropy "wins" in the competition with the exchange anisotropy and thus rotates SkX by an angle of 30°.

In summary, we have established a novel model to explain the continuous rotation of SkX under the electric field. In this model, SkX is deformable, and the anisotropies considered are the exchange and fourth order anisotropies. We also find that the electric field along the crystal direction leads to first or second order rotational transition of SkX, depending on whether it is in the $(1\bar{1}0)$ plane.

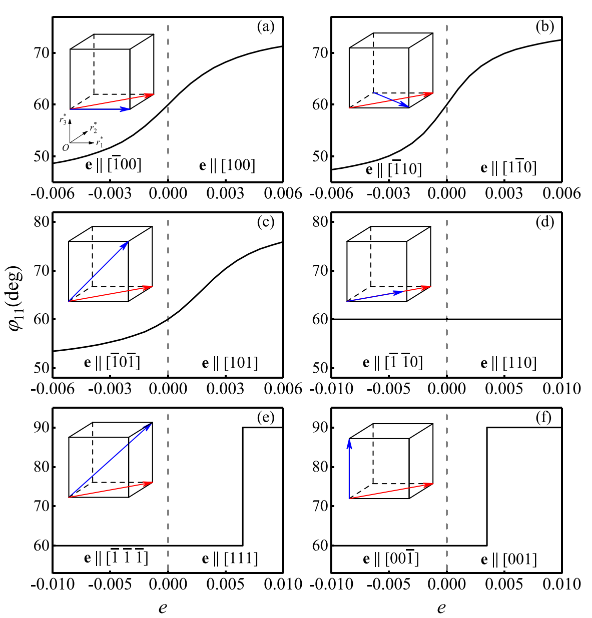

FIG. 4. Rotations of SkX under the electric field parallel to (a) [100], (b) $[1\bar{1}0]$, (c) [101], (d) [110], (e) [111], and (f) [001]. For (a)–(c), $-0.006 < e < 0.006$; for (d)–(f), $-0.01 < e < 0.01$. The red and blue arrows in the insets indicate the directions of the magnetic field and electric field, respectively.

This work was supported by the NSFC (National Natural Science Foundation of China) through fund Nos. 11772360, 11832019, and 11572355, the Guangdong Basic and Applied Basic Research Foundation (Grant No. 2019A1515012016), and the Pearl River Nova Program of Guangzhou (Grant No. 201806010134).

REFERENCES

[1]S. Mühlbauer, B. Binz, F. Jonietz, C. Pfleiderer, A. Rosch, A. Neubauer, R. Georgii, and P. Böni, Science **323**, 915 (2009).
[2]F. Jonietz, S. Mühlbauer, C. Pfleiderer, A. Neubauer, W. Münzer, A. Bauer, T. Adams, R. Georgii, P. Böni, R. A. Duine *et al.*, Science **330**, 1648 (2010).
[3]X. Yu, N. Kanazawa, W. Zhang, T. Nagai, T. Hara, K. Kimoto, Y. Matsui, Y. Onose, and Y. Tokura, Nat. Commun. **3**, 988 (2012).
[4]X. Zhang, G. Zhao, H. Fangohr, J. P. Liu, W. Xia, J. Xia, and F. Morvan, Sci. Rep. **5**, 7643 (2015).
[5]I. Dzyaloshinsky, J. Phys. Chem. Solids **4**, 241 (1958).

[6]Y. Hu and X. Wan, arXiv:1905.02165 (2019).
[7]X. Yu, N. Kanazawa, Y. Onose, K. Kimoto, W. Zhang, S. Ishiwata, Y. Matsui, and Y. Tokura, Nat. Mater. **10**, 106 (2011).
[8]X. Yu, Y. Onose, N. Kanazawa, J. Park, J. Han, Y. Matsui, N. Nagaosa, and Y. Tokura, Nature **465**, 901 (2010).
[9]T. Adams, A. Chacon, M. Wagner, A. Bauer, G. Brandl, B. Pedersen, H. Berger, P. Lemmens, and C. Pfleiderer, Phys. Rev. Lett. **108**, 237204 (2012).
[10]S. Seki, X. Yu, S. Ishiwata, and Y. Tokura, Science **336**, 198 (2012).
[11]Y. Tokunaga, X. Yu, J. White, H. M. Rønnow, D. Morikawa, Y. Taguchi, and Y. Tokura, Nat. Commun. **6**, 7638 (2015).
[12]I. Kézsmárki, S. Bordács, P. Milde, E. Neuber, L. Eng, J. White, H. M. Rønnow, C. Dewhurst, M. Mochizuki, K. Yanai *et al.*, Nat. Mater. **14**, 1116 (2015).
[13]Y. Fujima, N. Abe, Y. Tokunaga, and T. Arima, Phys. Rev. B **95**, 180410 (2017).
[14]T. Kurumaji, T. Nakajima, V. Ukleev, A. Feoktystov, T-h Arima, K. Kakurai, and Y. Tokura, Phys. Rev. Lett. **119**, 237201 (2017).
[15]R. Takagi, J. White, S. Hayami, R. Arita, D. Honecker, H. Rønnow, Y. Tokura, and S. Seki, Sci. Adv. **4**, eaau3402 (2018).
[16]A. K. Nayak, V. Kumar, T. Ma, P. Werner, E. Pippel, R. Sahoo, F. Damay, U. K. Rößler, C. Felser, and S. S. Parkin, Nature **548**, 561 (2017).
[17]L. J. Bannenberg, H. Wilhelm, R. Cubitt, A. Labh, M. P. Schmidt, E. Lelièvre-Berna, C. Pappas, M. Mostovoy, and A. O. Leonov, npj Quantum Mater. **4**, 11 (2019).
[18]F. Qian, L. J. Bannenberg, H. Wilhelm, G. Chaboussant, L. M. Debeer-Schmitt, M. P. Schmidt, A. Aqeel, T. T. Palstra, E. Brück, A. J. Lefering *et al.*, Sci. Adv. **4**, eaat7323 (2018).
[19]M. Halder, A. Chacon, A. Bauer, W. Simeth, S. Mühlbauer, H. Berger, L. Heinen, M. Garst, A. Rosch, and C. Pfleiderer, Phys. Rev. B **98**, 144429 (2018).
[20]A. Chacon, L. Heinen, M. Halder, A. Bauer, W. Simeth, S. Mühlbauer, H. Berger, M. Garst, A. Rosch, and C. Pfleiderer, Nat. Phys. **14**, 936 (2018).
[21]X. Wan, Y. Hu, and B. Wang, Phys. Rev. B **99**, 180406 (2019).
[22]S. Zhang, W. Wang, D. Burn, H. Peng, H. Berger, A. Bauer, C. Pfleiderer, G. van der Laan, and T. Hesjedal, Nat. Commun. **9**, 2115 (2018).
[23]K. Shibata, J. Iwasaki, N. Kanazawa, S. Aizawa, T. Tanigaki, M. Shirai, T. Nakajima, M. Kubota, M. Kawasaki, H. Park *et al.*, Nat. Nanotechnol. **10**, 589 (2015).
[24]L. Kong and J. Zang, Phys. Rev. Lett. **111**, 067203 (2013).
[25]J. S. White, I. Levatić, A. Omrani, N. Egetenmeyer, K. Prša, I. Živković, J. L. Gavilano, J. Kohlbrecher, M. Bartkowiak, H. Berger *et al.*, J. Phys.: Condens. Matter **24**, 432201 (2012).
[26]Y.-H. Liu, Y.-Q. Li, and J. H. Han, Phys. Rev. B **87**, 100402 (2013).
[27]Y. Okamura, F. Kagawa, S. Seki, and Y. Tokura, Nat. Commun. **7**, 12669 (2016).
[28]J. White, I. Živković, A. Kruchkov, M. Bartkowiak, A. Magrez, and H. Rønnow, Phys. Rev. Appl. **10**, 014021 (2018).
[29]J. White, K. Prša, P. Huang, A. Omrani, I. Živković, M. Bartkowiak, H. Berger, A. Magrez, J. Gavilano, G. Nagy *et al.*, Phys. Rev. Lett. **113**, 107203 (2014).
[30]W. Münzer, A. Neubauer, T. Adams, S. Mühlbauer, C. Franz, F. Jonietz, R. Georgii, P. Böni, B. Pedersen, M. Schmidt *et al.*, Phys. Rev. B **81**, 041203 (2010).
[31]Y. Luo, S.-Z. Lin, D. M. Fobes, Z. Liu, E. D. Bauer, J. B. Betts, A. Migliori, J. D. Thompson, M. Janoschek, and B. Maiorov, Phys. Rev. B **97**, 104423 (2018).
[32]X. Wan, Y. Hu, and B. Wang, Phys. Rev. B **98**, 174427 (2018).
[33]S. Seki, S. Ishiwata, and Y. Tokura, Phys. Rev. B **86**, 060403 (2012).
[34]M. Belesi, I. Rousochatzakis, M. Abid, U. Rößler, H. Berger, and J.-P. Ansermet, Phys. Rev. B **85**, 224413 (2012).
[35]A. Kruchkov, J. White, M. Bartkowiak, I. Živković, A. Magrez, and H. Rønnow, Sci. Rep. **8**, 10466 (2018).
[36]M. Born and K. Huang, *Dynamical Theory of Crystal Lattices* (Clarendon Press, Oxford, 1954).
[37]L. Bannenberg, F. Qian, R. Dalgliesh, N. Martin, G. Chaboussant, M. Schmidt, D. L. Schlagel, T. A. Lograsso, H. Wilhelm, and C. Pappas, Phys. Rev. B **96**, 184416 (2017).
[38]K. Makino, J. D. Reim, D. Higashi, D. Okuyama, T. J. Sato, Y. Nambu, E. P. Gilbert, N. Booth, S. Seki, and Y. Tokura, Phys. Rev. B **95**, 134412 (2017).
[39]Y. Okamura, Y. Yamasaki, D. Morikawa, T. Honda, V. Ukleev, H. Nakao, Y. Murakami, K. Shibata, F. Kagawa, S. Seki *et al.*, Phys. Rev. B **96**, 174417 (2017).
[40]Y. Okamura, Y. Yamasaki, D. Morikawa, T. Honda, V. Ukleev, H. Nakao, Y. Murakami, K. Shibata, F. Kagawa, S. Seki *et al.*, Phys. Rev. B **95**, 184411 (2017).